A New Detection Method of Gravitational Waves

SIGN
(Stellar Interferometer for Gravitational wave)

IL H. PARK (SKKU, Korea)

NextGAPES-2019

Workshop on the Next Generation of AstroParticle Experiments in Space,
Lomonosov Moscow State University, on June 21-22, 2019

arXiv:1906.06018v1 (14 June 2019)

Stellar Interferometry for Detection of Gravitational Waves

I.H. Park,[1,*] D.H. Kim,[1] K.-Y. Choi,[1] and E. Won[2,†]

[1] *Department of Physics, Sungkyunkwan University (SKKU), Suwon, 16419, Republic of Korea*

[2] *Department of Physics, Korea University, Seoul, 02841, Republic of Korea*

We propose a new method to detect gravitational waves, based on spatial coherence interferometry using star light as opposed to conventional laser light. Two beams of light from a distant star are used in our space-borne experiment. In contrast to existing or proposed future gravitational-wave detectors where the plane of two laser beams are located orthogonal to the propagation direction of gravitational waves at the maximum response to gravitational waves, our stellar interferometer configures the direction of gravitational waves along the plane of two light beams. This configuration is expected to reduce noises in the low-frequency range significantly. Our proposed experiment would be complementary to on-going and planned gravitational-wave detectors such as laser interferometers and pulsar timing arrays, by covering the frequency range of $10^{-7} - 10^{-4}$ Hz of gravitational waves.

Wave & Particle Astronomy

- Constituent of the universe → wave & matter (visible & dark)
- How to probe & understand the universe (apart from theory) → wave & particle
- **"wave astronomy"** (EM and gravity only at large scale)
  - EM astronomy (optical, UV, IR, X, γ) → multi-wavelength now
  - GW astronomy → GW discovered in 2015 (GW150914)
- **"particle astronomy"** (why not)
- **GW170817 via GW & EM** → NS-NS merger & GRB & kilonova → **dawn of "multi-messenger astrophysics (MMA)"**
- **Future GW detectors** → **"multi-wavelength GW" astronomy**

Content

- Gravitational wave detectors
- Coherence experiments in interferometry
- Proposed method of SIGN
- Sensitivity of SIGN
- Technical challenge
- Conclusion

Detection of Gravitational Wave

- Resonant Acoustic Detectors
  - Bar detectors: Auriga(Italy), ALLEGRO(USA) …
  - Spherical detectors: Mini-Grail (Netherlands) …
  - Sensitive to order of kHz of GW
- Laser Interferometers
  - Ground Laser Interferometers: LIGO, VIRGO, KAGRA
  - Space Laser Interferometers: LISA, DECIGO …
- Pulsar Timing Arrays
  - Maximize the sensitivity to relatively low-frequency hum of colliding supermassive black holes
  - Parkes PTA (Australia), NANOGrav (North America), European PTA (Europe), SKA … → dozens of pulsars
- CMB polarization
  - Preserved the space stretched/squeezed by Inflation
  - BICEP2 mistook dust in the Milky Way for its quarry
- Others
  - Doppler tracking, Atom interferometer …
  - **Stellar Interferometer** in this talk

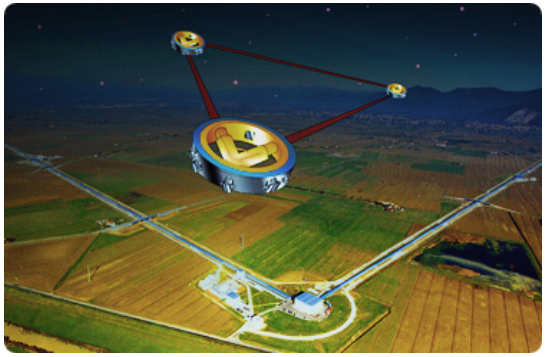

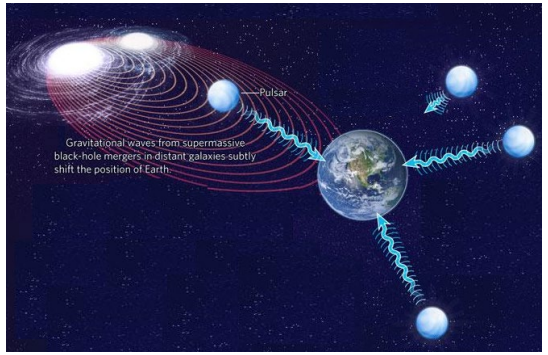

Frequency range: 10^{-18} ~ 10^{8} Hz

potential sources of GW

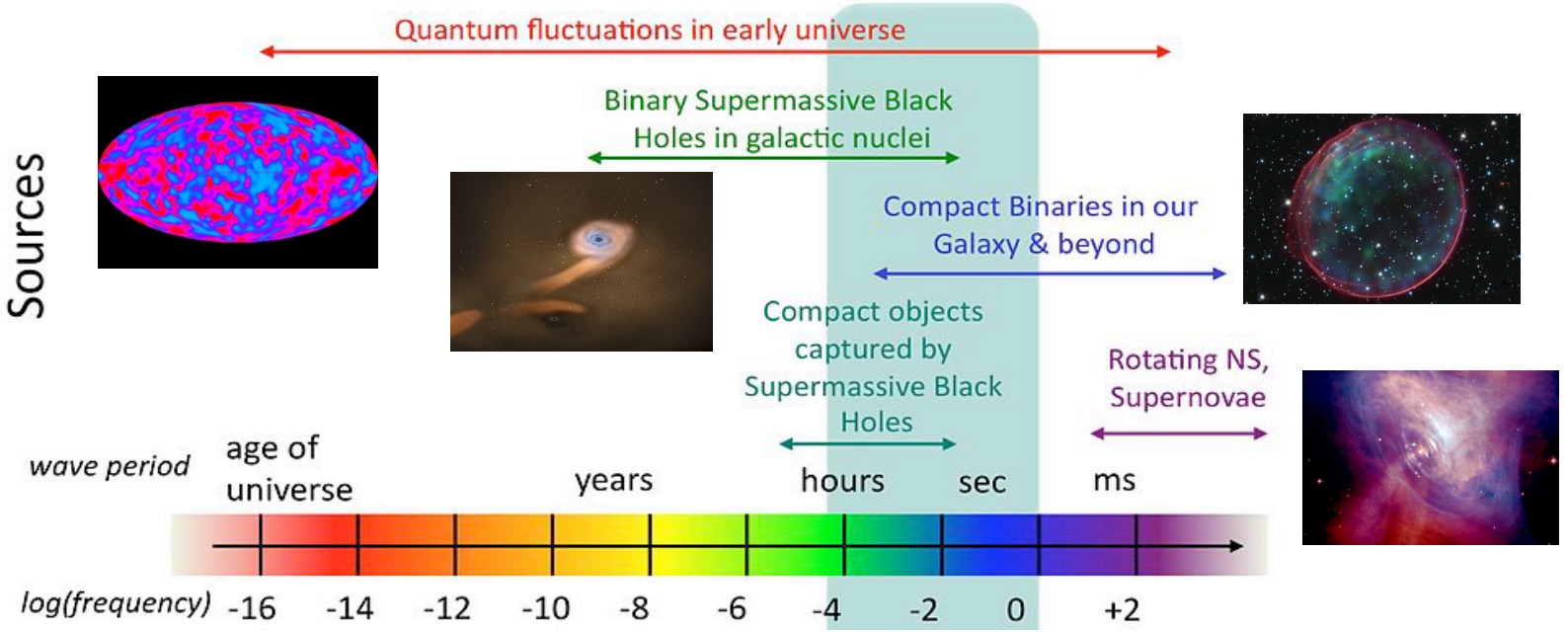

the range of freq to which different detectors are sensitive

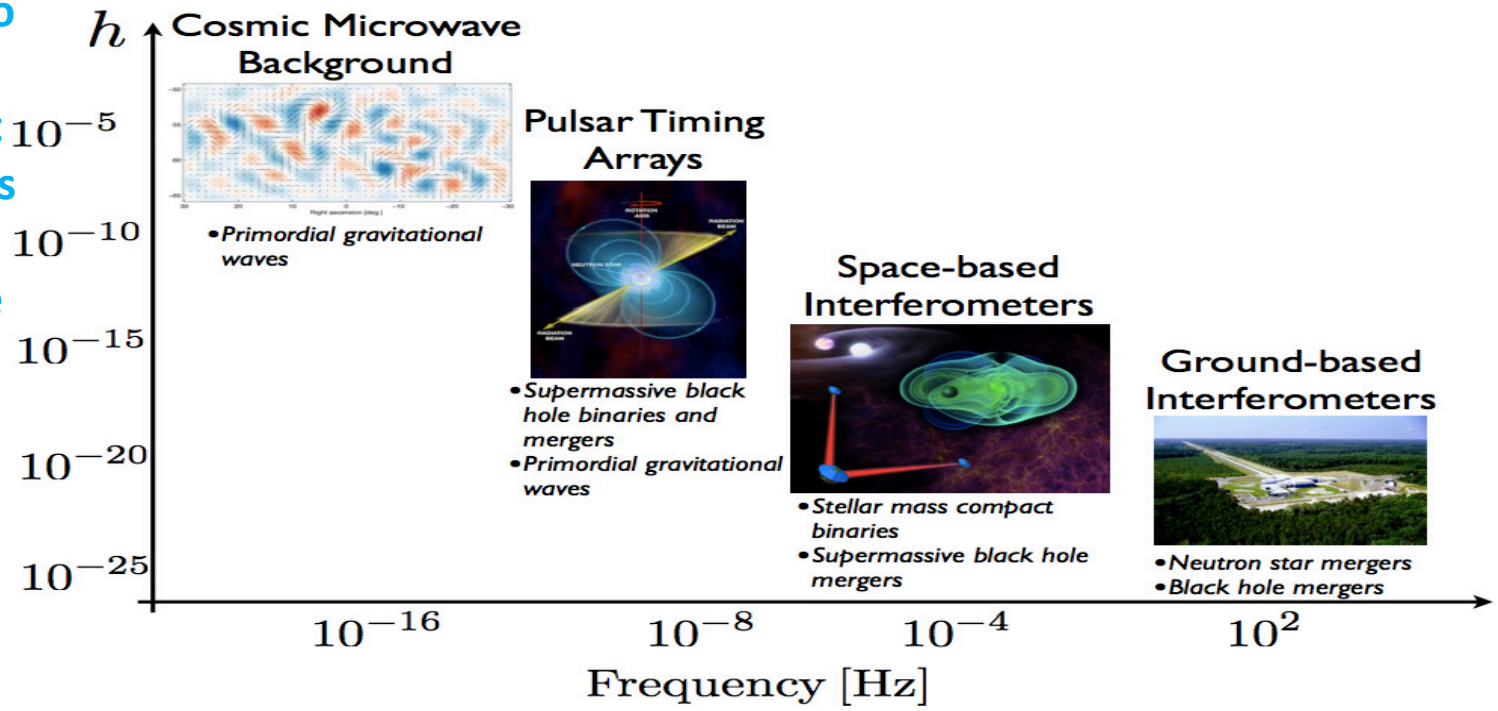

Coherence Experiments (two types)

Coherence?

- Measure of the correlation between the phases measured at **temporally or spatially** different points on a wave

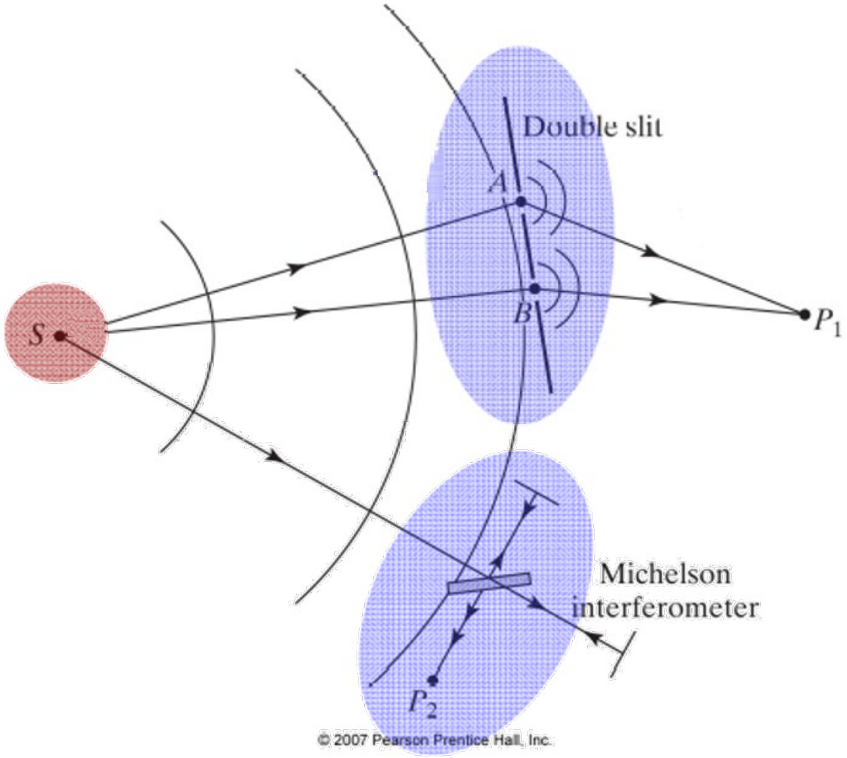

Spatial coherence(lateral coherence):
… difference at points transverse to the direction of propagation showing how uniform the phase of the wavefront is (size of the source)

Temporal coherence(longitudinal):
… difference at points along the direction of propagation showing how monochromatic a source is (spectral purity of the source)

Fringe visibility: $l_t = c\tau_t = \frac{c}{\Delta\nu} \geq SAP_1 - SBP_1$

coherence length **coherence time** **Path length difference**

Spatial Coherence

- If extended source, fringe visibility depends on l_s
- Consider two fringe systems

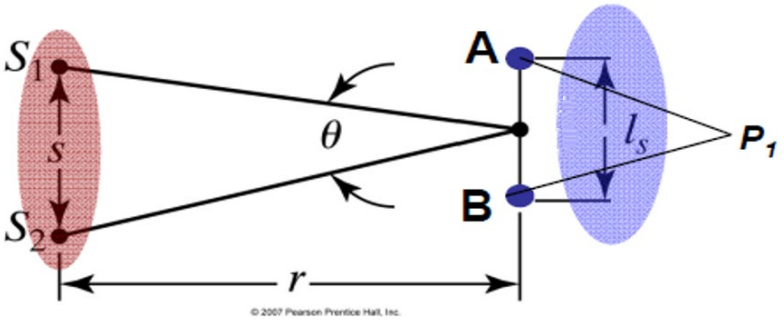

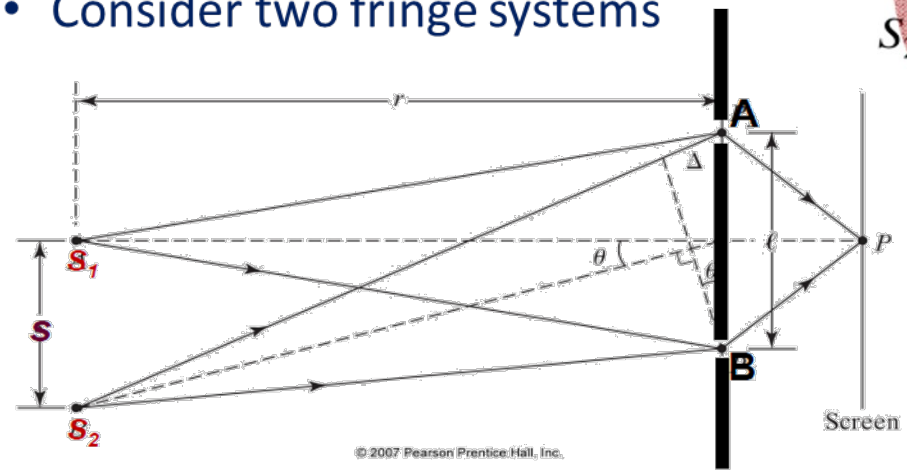

$$S_2A - S_2B = \Delta = \frac{\lambda}{2} \approx l\theta = \frac{l \cdot s}{r}$$

- For a continuous source

$$l = l_s \cong \frac{\lambda}{\theta} = \frac{r\lambda}{s} \rightarrow \text{Spatial coherence width of an extended source}$$

- If circular source,

$$l_s = \frac{1.22\,\lambda}{\theta}$$

Separation is bigger for smaller viewing angle of source.

Coherence Experiments (two types)

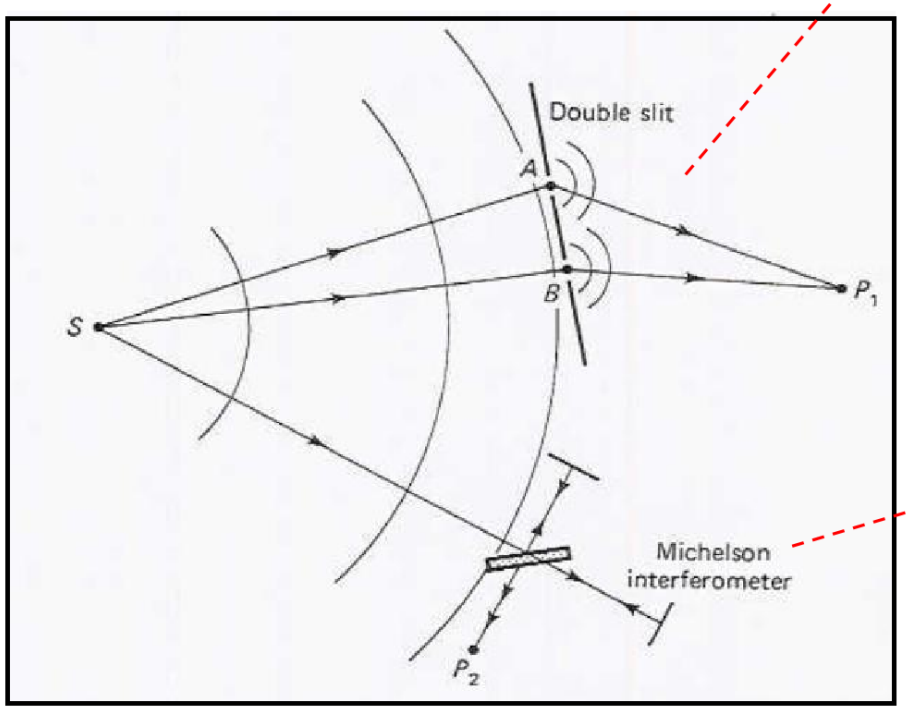

Spatial Coherence ➡ SIGN

coherence length is inversely proportional to size

- Spatial extent of the source
- used for measuring angular diameters
- Basis for **stellar interferometry,** widely used these days for imaging of astrophysics objects

Temporal Coherence ➡ LIGO, LISA

- Spectral purity, coherence time $\tau_c \approx 1/\Delta\nu$
- Laser has large τ_c up to some µs, while white light in the order of fs
- **Michelson interferometer**

Stellar Interferometer (1920)

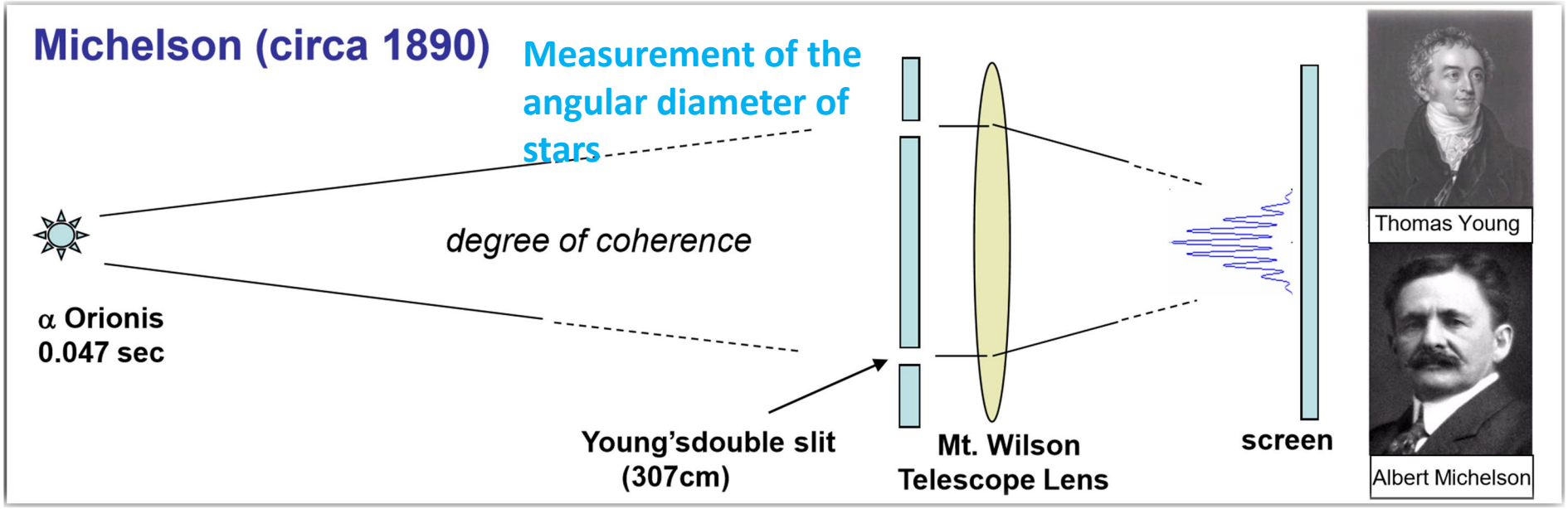

Concept of SIGN (2018)

measurement of GW intervention on spatial interferometer

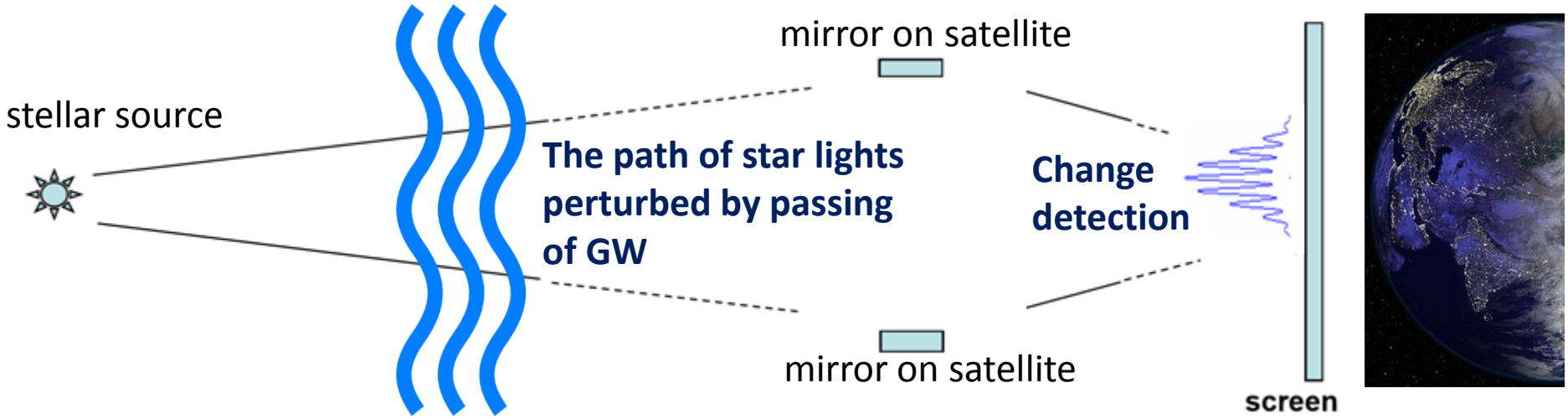

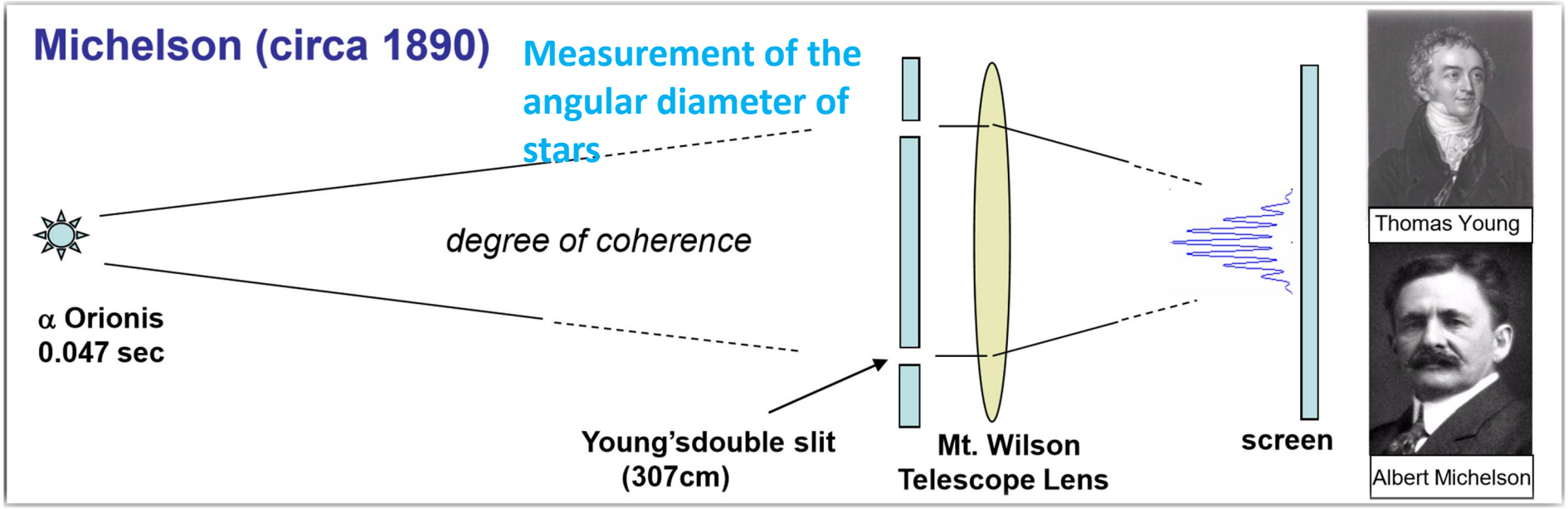

SIGN (Stellar Interferometer for Gravitational wave)

MEASUREMENT OF THE DIAMETER OF α ORIONIS WITH THE INTERFEROMETER[1]

By A. A. MICHELSON and F. G. PEASE

ABSTRACT

Twenty-foot interferometer for measuring minute angles.—Since pencils of rays at least 10 feet apart must be used to measure the diameters of even the largest stars, and because the interferometer results obtained with the 100-inch reflector were so encouraging, the construction of a 20-foot interferometer was undertaken. A very rigid beam made of structural steel was mounted on the end of the Cassegrain cage, and four 6-inch mirrors were mounted on it so as to reduce the separation of the pencils to 45 inches and enable them to be brought to accurate coincidence by the telescope. The methods of making the fine adjustments necessary are described, including the use of two thin wedges of glass to vary continuously the equivalent air-path of one pencil. Sharp fringes were obtained with this instrument in August, 1920.

Diameter of α Orionis.—Although the interferometer was not yet provided with means for continuously altering the distance between the pencils used, some observations were made on this star, which was known to be very large. On December 13, 1920, with very good seeing, no fringes could be found when the separation of the pencils was 121 inches, although tests on other stars showed the instrument to be in perfect adjustment. This separation for minimum visibility gives the angular diameter as 0″.047 within 10 per cent, assuming the disk of the star uniformly luminous. Hence, taking the parallax as 0″.018, the linear diameter comes out 240×10^6 miles.

Interferometer method of determining the distribution of luminosity on a stellar disk.—The variation of intensity of the interference fringes with the separation of the two pencils depends not only on the angular diameter of the disk but also on the distribution of luminosity. The theory is developed for the case in which $I = I_0 (R^2 - r^2)^n$, and formulae are given for determining n from observations.

Table of values of $\int_0^1 (1-x^2)^{n+\frac{1}{2}} \cos kx\, dx$, for n equal to 0, $\frac{1}{2}$, 1, and 2, and for k up to 600°, is given.

It was shown in *Contributions* Nos. 184 and 185,[2] that the application of interference methods to astronomical measurements is not seriously affected by atmospheric disturbances, and indeed observations by these methods have proved feasible even when the seeing was very poor. The explanation of this apparent paradox lies in the fact that when the whole objective is effective, the atmospheric disturbances, being irregularly distributed over the surface, simply blur the diffraction pattern; but in the case of two isolated pencils too small to be affected by such an integrated disturbance, the resulting interference fringes, though in motion,

[1] *Contributions from the Mount Wilson Observatory*, No. 203.

[2] *Astrophysical Journal*, **51**, 257, 263, 1920.

are quite distinct, unless the period of the disturbances is too rapid for the eye to follow.

When it was found that the interference fringes remain at full visibility with the slits separated by the diameter of the 100-inch mirror, it was decided to build an interferometer with movable outer mirrors (Fig. 1) in order to make tests with separations as great as 20 feet.

The interferometer beam (Plate IV*a* and Fig. 2) was made of structural steel, as stiff and rigid as circumstances of weight and

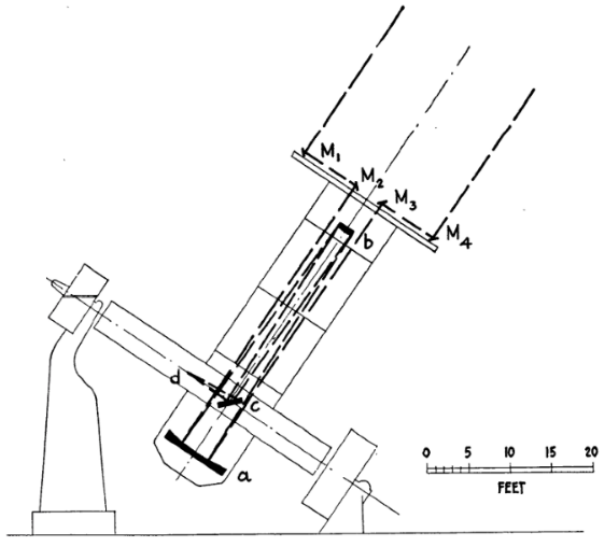

FIG. 1.—Diagram of optical path of interferometer pencils. M_1, M_2, M_3, M_4, mirrors; *a*, 100-inch paraboloid; *b*, convex mirror; *c*, coudé flat; *d*, focus.

operation would permit, for flexure causes a separation of the two pencils, and any vibration as great as one-thousandth of a millimeter blurs the fringes.

The beam is constructed of two 10-inch channels with flanges turned inward, separated by pieces of 12-inch channel and covered on the bottom with $\frac{3}{16}$-inch (4.75 mm) steel plate (*C*, Fig. 2), all riveted securely together.

To reduce the weight holes were cut wherever the removal of metal would not cause a weakening of the structure. The inner edges of the top flanges were planed true to 0.001 of an inch

Michelson Stellar Interferometer (1920)

First direct measurement of stellar diameter with the a telescope at Mount Wilson (α-Orionis)

PLATE IV

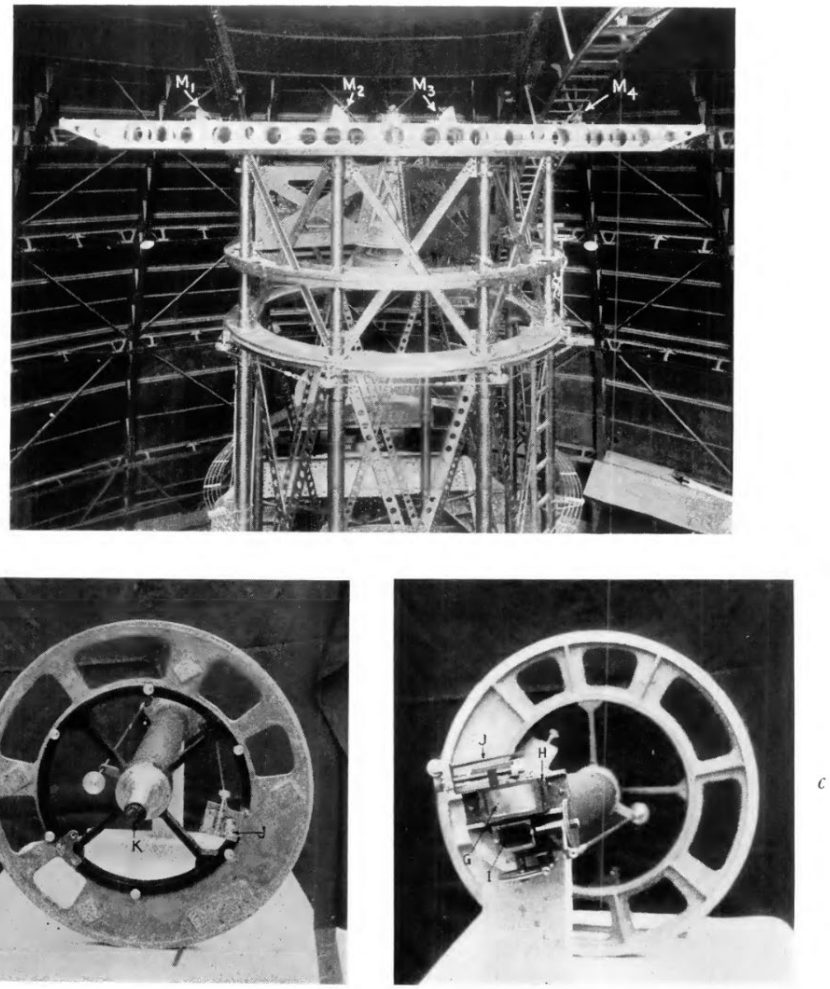

INTERFEROMETER USED WITH 100-INCH HOOKER REFLECTOR

a. *A*, 20-foot interferometer beam on end of telescope; M_1, M_2, M_3, M_4, mirrors; *D*, Cassegrain cage
b, *c*. Adapter at focus; *J*, rod to shift wedge; *K*, direct-vision prism; *G*, fixed wedge; *H*, movable wedge; *I*, plane-parallel compensator.

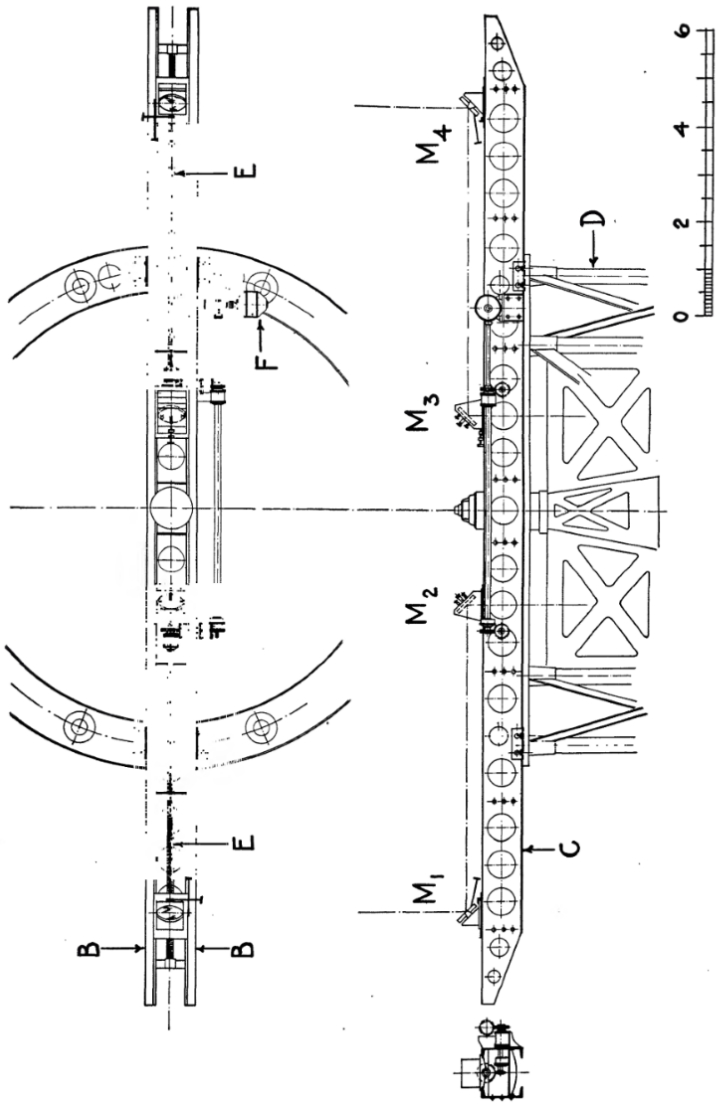

FIG. 2.—Diagram of 20-foot interferometer beam. M_1, M_2, M_3, M_4, mirrors; *B*, *B*, 10-inch channels; *C*, steel plate; *E*, *E*, screws to move outer mirrors; *F*, motor drive for screws; *D*, Cassegrain cage.

Michelson Stellar Int.(1920) → SIGN(2018)

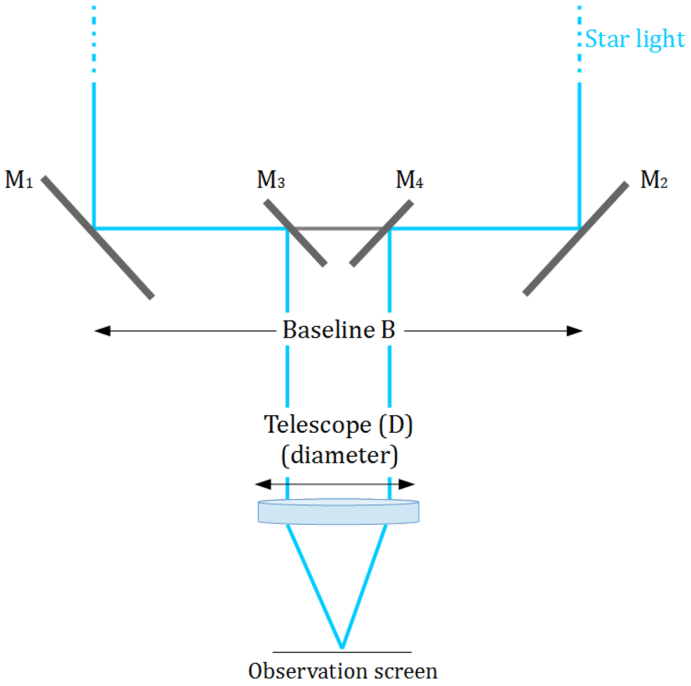

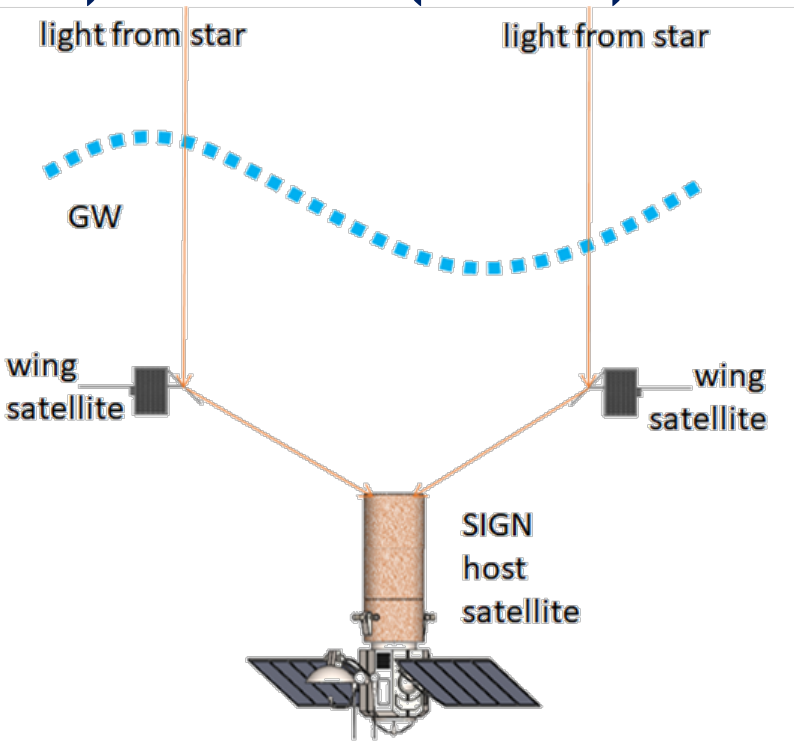

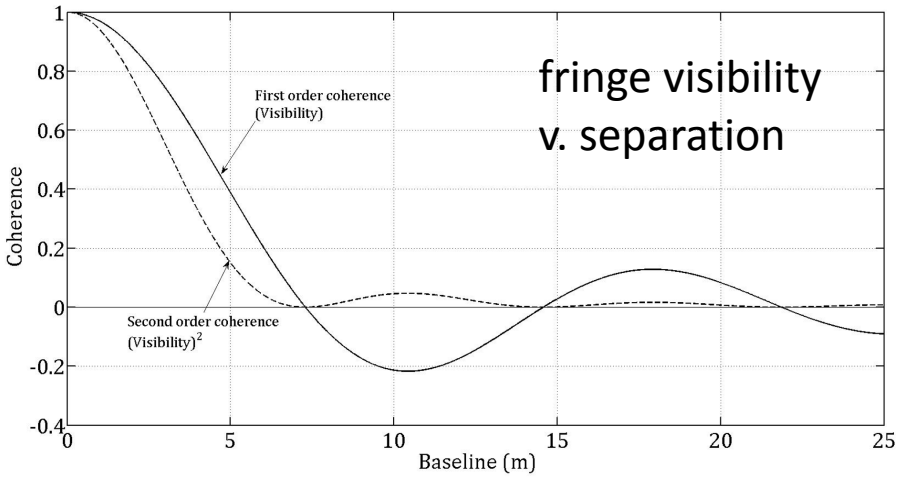

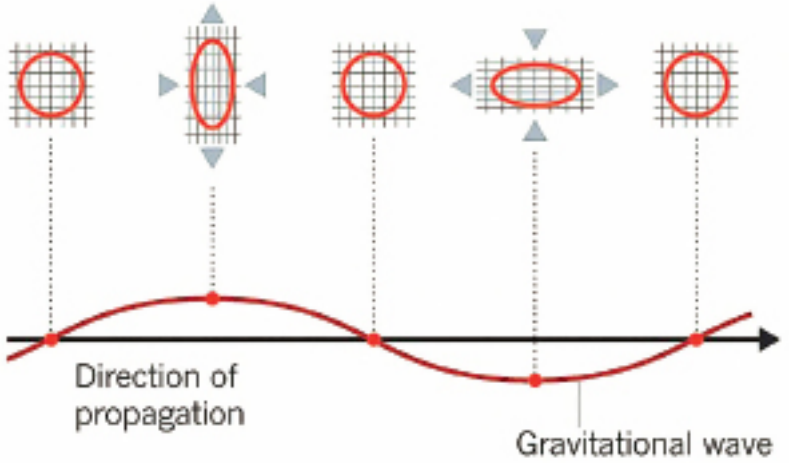

Two satellites option: Tandem operation

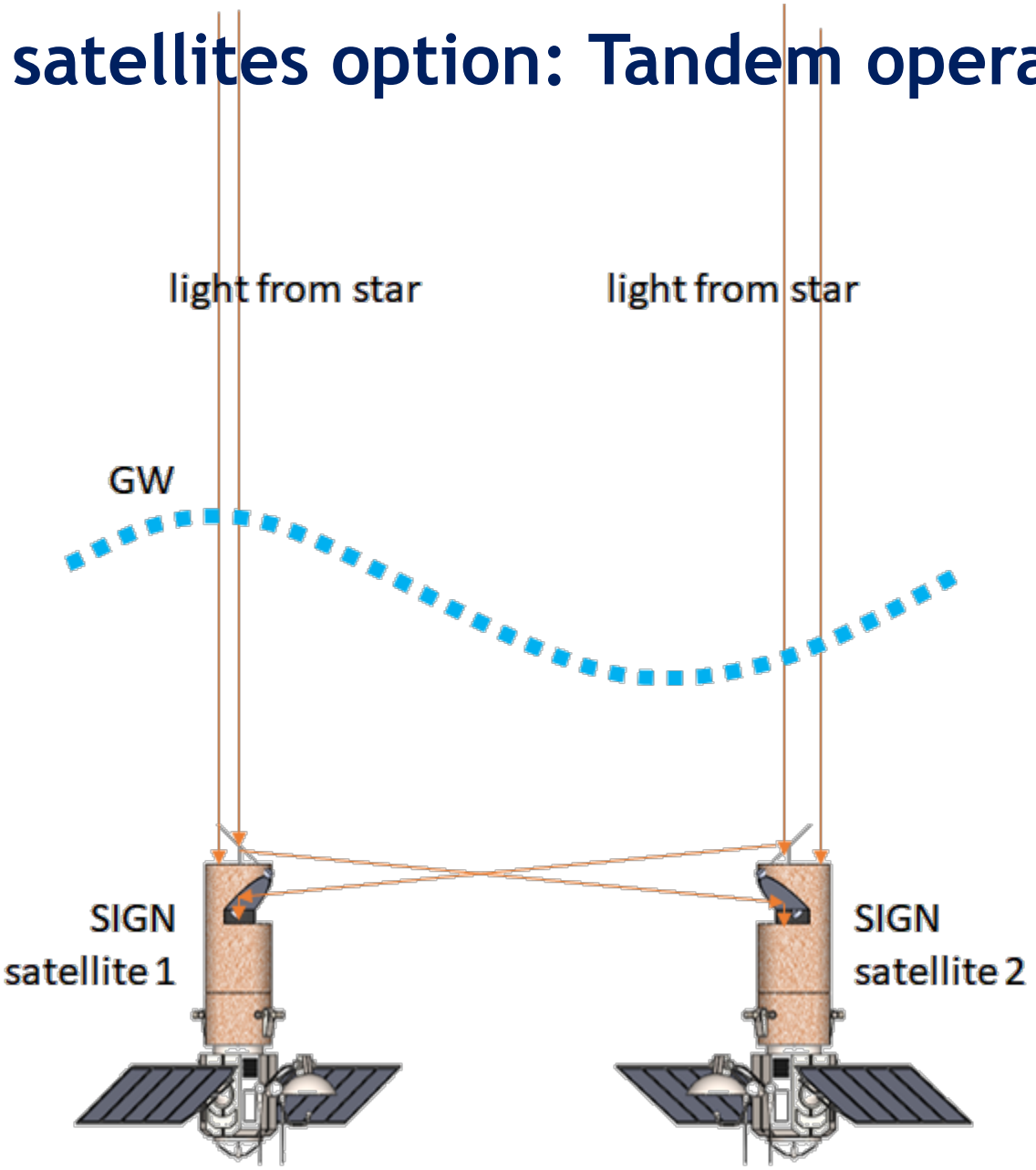

Comparison among LIGO, LISA, and SIGN

LIGO and LISA: A gravitational wave propagates normal to the interferometer plane
SIGN: it travels in the direction of the interferometer plane of two parallel EM lights

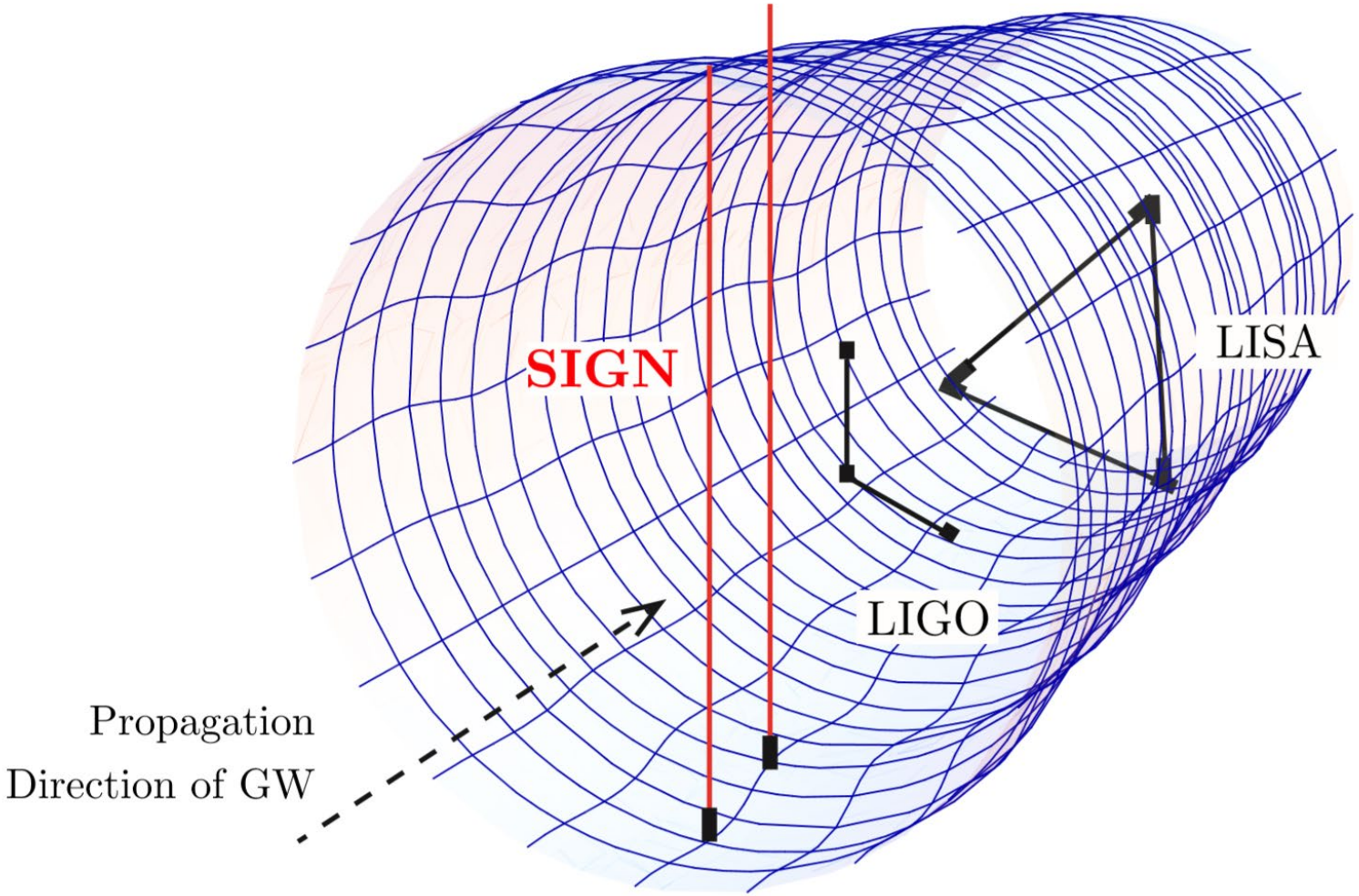

Candidates of Stellar Sources for SIGN

Major concerns are of coherent length, size, distance, apparant magnitude

star	λ_{EM} (μm)	size of star (times Sun)	distance to star (Ly)	θ_s (μarcsec)	l_s (km)	sun seeing size (m)	apparent mag
SPICA	0.6	7.4	262	428.40	0.352		0.98
SPICA secondary	0.6	3.64	262	210.72	0.716		0.98
SMC AB8	0.6	2	197000	0.15	1000		12.83
WR1	0.6	1.33	11000	1.79	84		10.54
WR2	0.6	0.89	8200	1.60	94		11.33
R136a1	0.6	30	163000	2.72	55		12.23
Sun point (.1marcsec)	0.6	1	1.58E-05	100	5	15	~10

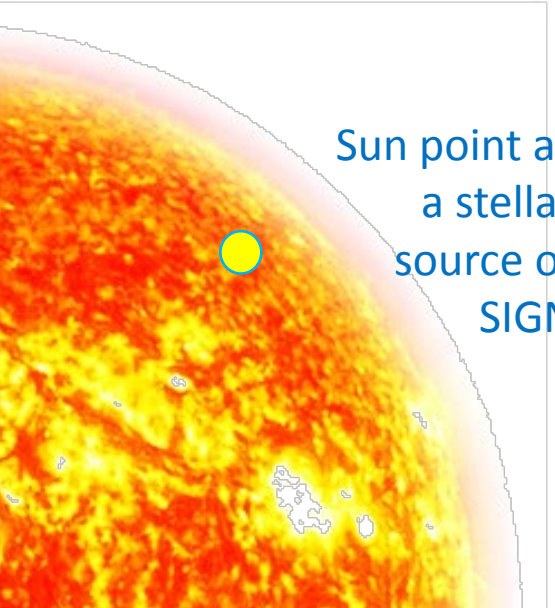

Sun point as a stellar source of SIGN

SMC AB8

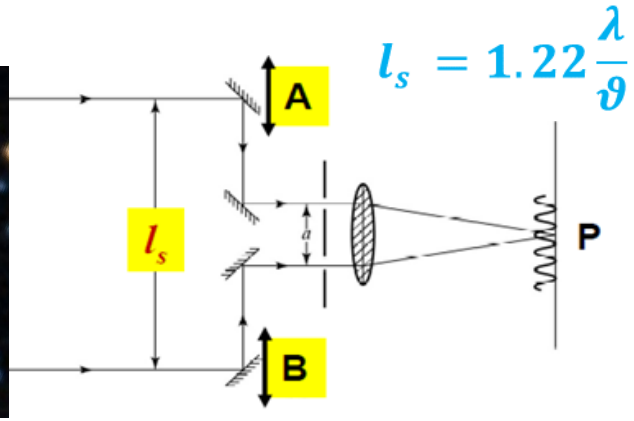

$$l_s = 1.22\frac{\lambda}{\vartheta}$$

(to be published elsewhere)

Path length difference in SIGN

Interference of light rays

$$
\begin{aligned}
(E_{\rm I}+E_{\rm II})_{\rm (con/des)} \approx\ & (\mathcal{E}_{\rm I}\pm\mathcal{E}_{\rm II})\exp\left[{\rm i}\left(KL_{\rm I}-\omega_{\rm EM}t-\pi/2\right)\right] \\
& + \left[\mathcal{E}_{\rm I}\exp\left({\rm i}\frac{1}{2}kl_{\rm s}\cos\phi\cos\theta\right)\pm\mathcal{E}_{\rm II}\exp\left(-{\rm i}\frac{1}{2}kl_{\rm s}\cos\phi\cos\theta\right)\right] \\
& \times\frac{h_{+}\omega_{\rm EM}\left(\sin^2\phi\sin^2\theta-\cos^2\theta\right)+2{\rm i}h_{\times}\omega_{\rm EM}\sin\phi\cos\theta\sin\theta}{2\omega_{\rm GW}\left(1-\cos\phi\sin\theta\right)} \\
& \times\exp\left[{\rm i}\left(KL_{\rm I}-\left(\omega_{\rm EM}+\omega_{\rm GW}\right)t-\pi/2\right)\right].
\end{aligned}
$$

Intensity of superposed light waves

$$
\begin{aligned}
\mathcal{I}_{\rm (con/des)} &= (E_{\rm I}+E_{\rm II})\,(E_{\rm I}+E_{\rm II})^{*} \\
&\approx (\mathcal{E}_{\rm I}\pm\mathcal{E}_{\rm II})^2 \\
&\quad+\left[\frac{h_{+}\omega_{\rm EM}}{\omega_{\rm GW}}\frac{\sin^2\phi\sin^2\theta-\cos^2\theta}{1-\cos\phi\sin\theta}(\mathcal{E}_{\rm I}\pm\mathcal{E}_{\rm II})^2\cos\left(\frac{1}{2}kl_{\rm s}\cos\phi\cos\theta\right)\right. \\
&\quad\left.-\frac{2h_{\times}\omega_{\rm EM}}{\omega_{\rm GW}}\frac{\sin\phi\cos\theta\sin\theta}{1-\cos\phi\sin\theta}(\mathcal{E}_{\rm I}^2-\mathcal{E}_{\rm II}^2)\sin\left(\frac{1}{2}kl_{\rm s}\cos\phi\cos\theta\right)\right]\times\cos\left(\omega_{\rm GW}t\right) \\
&\quad+\left[\frac{h_{+}\omega_{\rm EM}}{\omega_{\rm GW}}\frac{\sin^2\phi\sin^2\theta-\cos^2\theta}{1-\cos\phi\sin\theta}(\mathcal{E}_{\rm I}^2-\mathcal{E}_{\rm II}^2)\sin\left(\frac{1}{2}kl_{\rm s}\cos\phi\cos\theta\right)\right. \\
&\quad\left.+\frac{2h_{\times}\omega_{\rm EM}}{\omega_{\rm GW}}\frac{\sin\phi\cos\theta\sin\theta}{1-\cos\phi\sin\theta}(\mathcal{E}_{\rm I}\pm\mathcal{E}_{\rm II})^2\cos\left(\frac{1}{2}kl_{\rm s}\cos\phi\cos\theta\right)\right]\times\sin\left(\omega_{\rm GW}t\right)+\mathcal{O}\left(h^2\right)
\end{aligned}
$$

For $\theta=\varphi=0$, GW crosses EM light rays at a right angle by propagating in the *z*-direction while being polarized in the *xy*-plane

$$
\begin{aligned}
\mathcal{I}_{\rm (con/des)} &\approx (\mathcal{E}_{\rm I}\pm\mathcal{E}_{\rm II})^2 \\
&\quad-\frac{h_{+}\omega_{\rm EM}}{\omega_{\rm GW}}\left[(\mathcal{E}_{\rm I}\pm\mathcal{E}_{\rm II})^2\cos\left(\frac{kl_{\rm s}}{2}\right)\cos\left(\omega_{\rm GW}t\right)+(\mathcal{E}_{\rm I}^2-\mathcal{E}_{\rm II}^2)\sin\left(\frac{kl_{\rm s}}{2}\right)\sin\left(\omega_{\rm GW}t\right)\right]+\mathcal{O}\left(h^2\right)
\end{aligned}
$$

Simulation of EM perturbed by GW

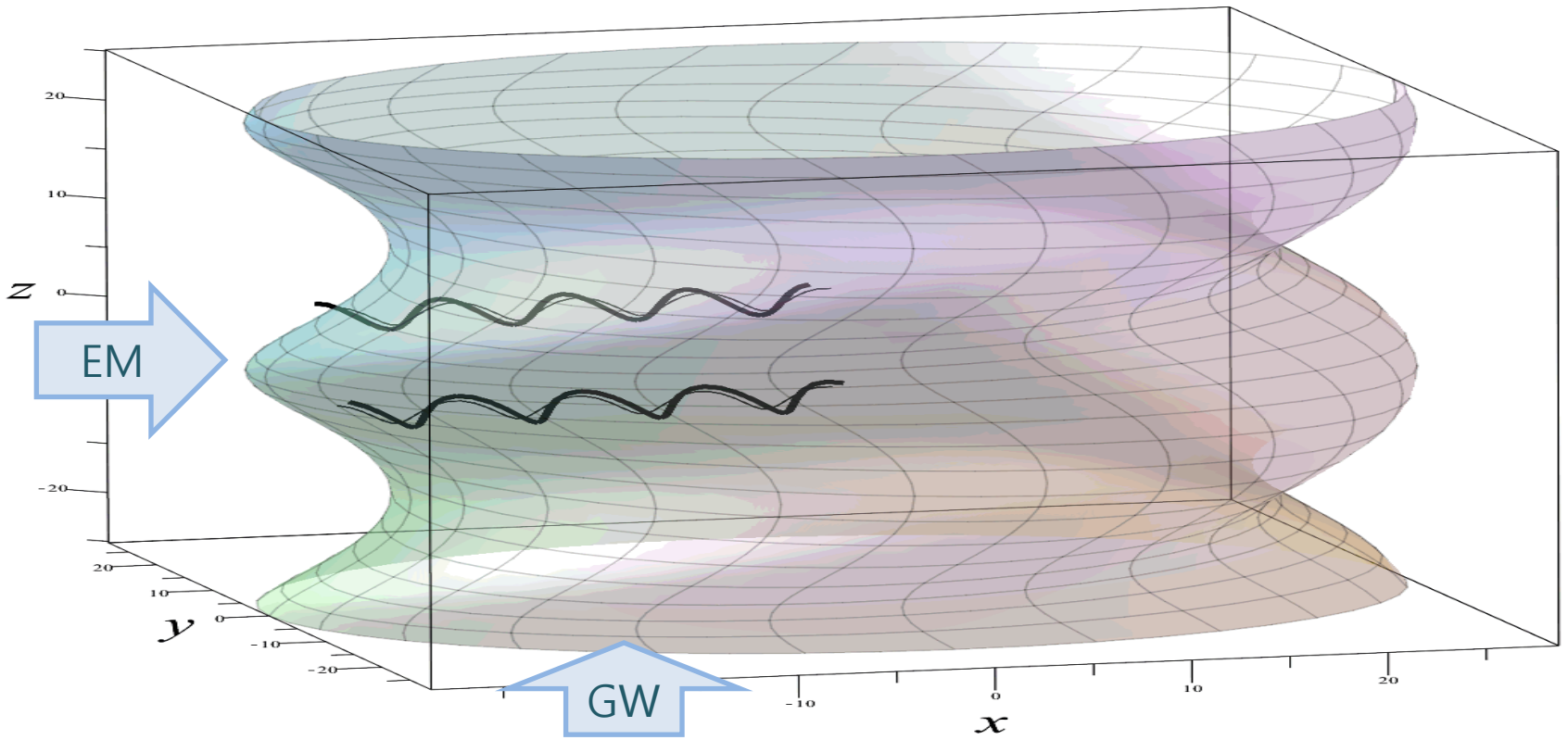

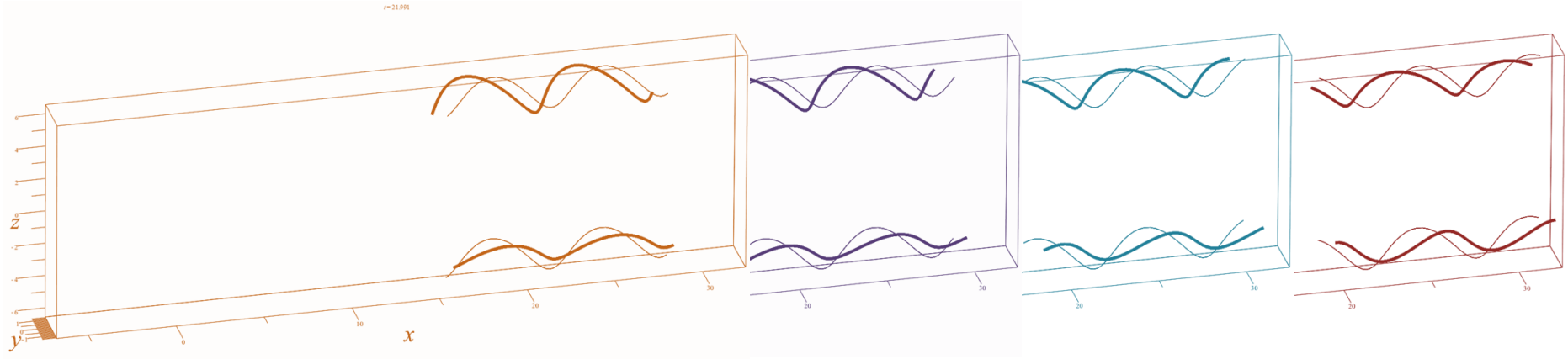

Response of the SIGN detector

Response function $R(f) \approx \dfrac{8}{15\left(1+\frac{2}{21}\left(\frac{f}{f_*}\right)^2\right)}$

$$\mathcal{R}(f) = \frac{1}{4\pi^2}\int_0^{\pi} d\psi \int_0^{2\pi} d\phi \int_0^{\pi} d\theta \, \sin\theta \left[F^{+}(f)\,F^{+*}(f) + F^{\times}(f)\,F^{\times *}(f)\right]$$

$$F^{+}(f) \equiv \frac{iA(\phi,\theta,\psi)}{1-\cos\phi\sin\theta\cos\psi-\sin\phi\sin\psi} \frac{\left[1-e^{i(1-\cos\phi\sin\theta\cos\psi-\sin\phi\sin\psi)f/f_\star}\right] e^{if/f_\star}}{f/f_\star}$$

$$F^{\times}(f) \equiv \frac{iB(\phi,\theta,\psi)}{1-\cos\phi\sin\theta\cos\psi-\sin\phi\sin\psi} \frac{\left[1-e^{i(1-\cos\phi\sin\theta\cos\psi-\sin\phi\sin\psi)f/f_\star}\right] e^{if/f_\star}}{f/f_\star}$$

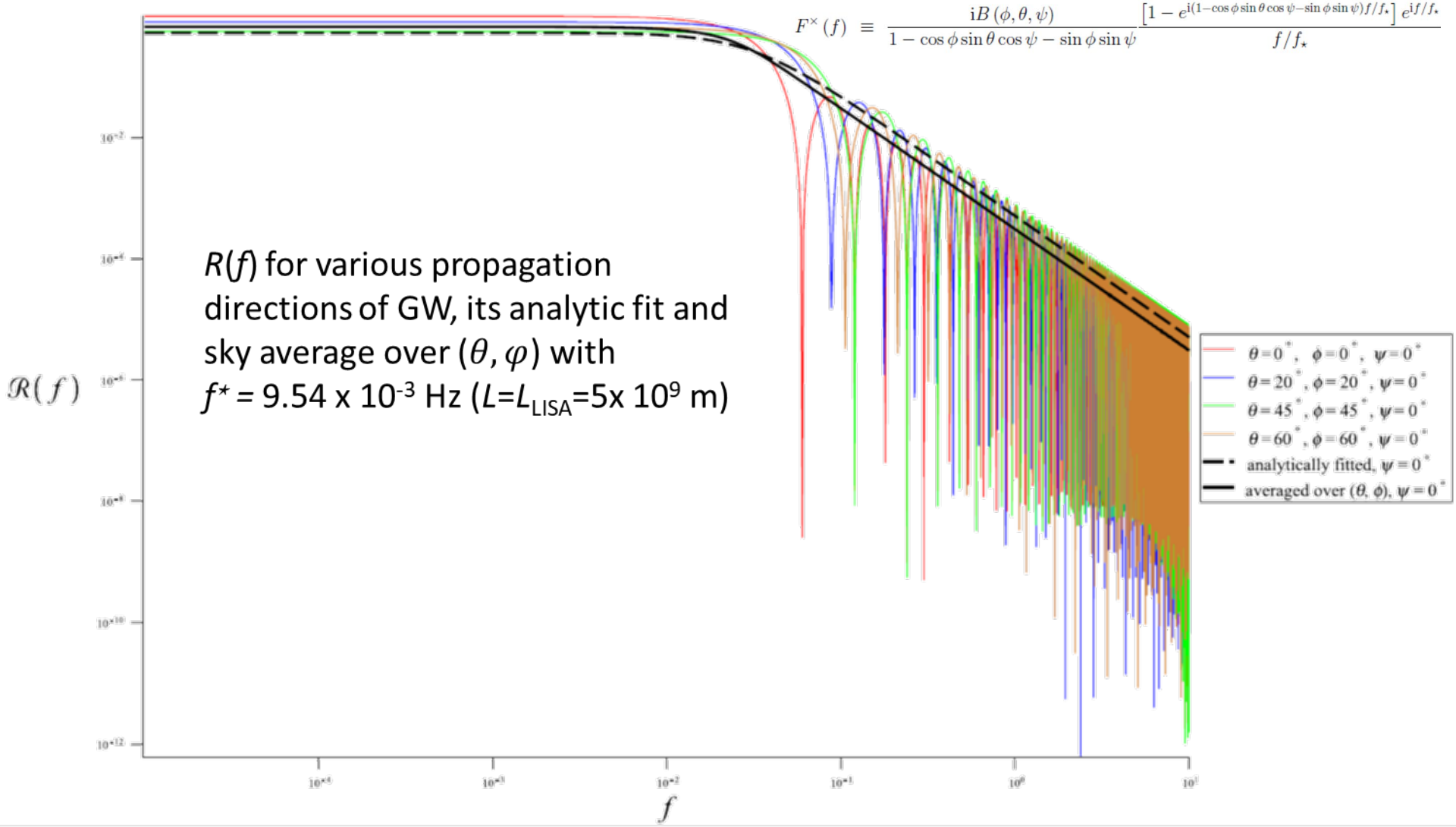

R(*f*) for various propagation directions of GW, its analytic fit and sky average over (θ, φ) with $f^\star = 9.54 \times 10^{-3}$ Hz ($L = L_{LISA} = 5 \times 10^9$ m)

Antenna patterns in long-wavelength approximation

$$F^{+}(f) \equiv \frac{\mathrm{i}A(\phi,\theta,\psi)}{1-\cos\phi\sin\theta\cos\psi-\sin\phi\sin\psi}\frac{\left[1-e^{\mathrm{i}(1-\cos\phi\sin\theta\cos\psi-\sin\phi\sin\psi)f/f_{\star}}\right]e^{\mathrm{i}f/f_{\star}}}{f/f_{\star}}$$

$$F^{\times}(f) \equiv \frac{\mathrm{i}B(\phi,\theta,\psi)}{1-\cos\phi\sin\theta\cos\psi-\sin\phi\sin\psi}\frac{\left[1-e^{\mathrm{i}(1-\cos\phi\sin\theta\cos\psi-\sin\phi\sin\psi)f/f_{\star}}\right]e^{\mathrm{i}f/f_{\star}}}{f/f_{\star}}$$

$\lim_{f\to 0}|F^{+}(\theta,\phi;f)|$

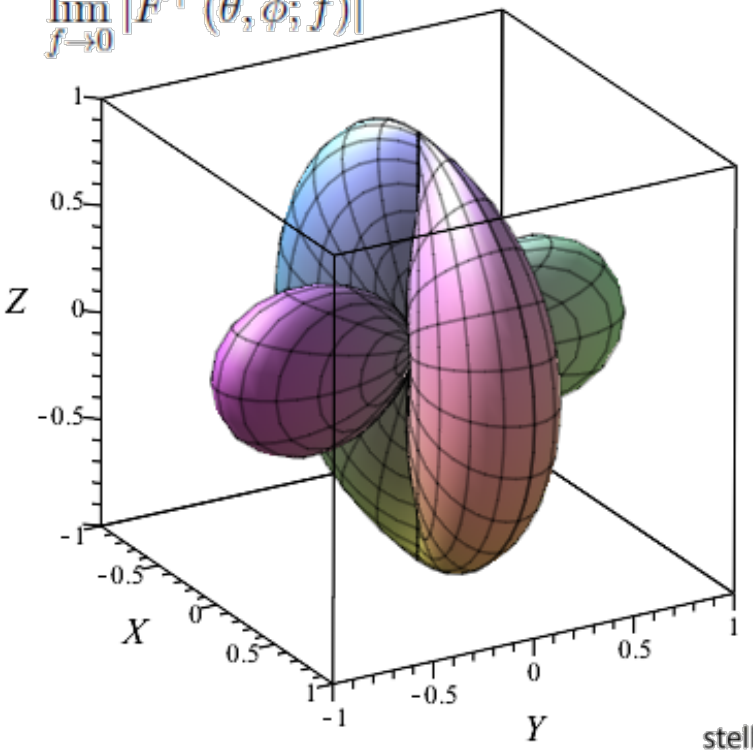

$\lim_{f\to 0}|F^{\times}(\theta,\phi;f)|$

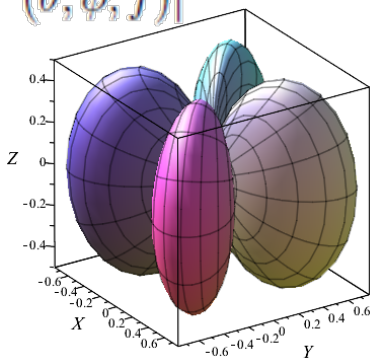

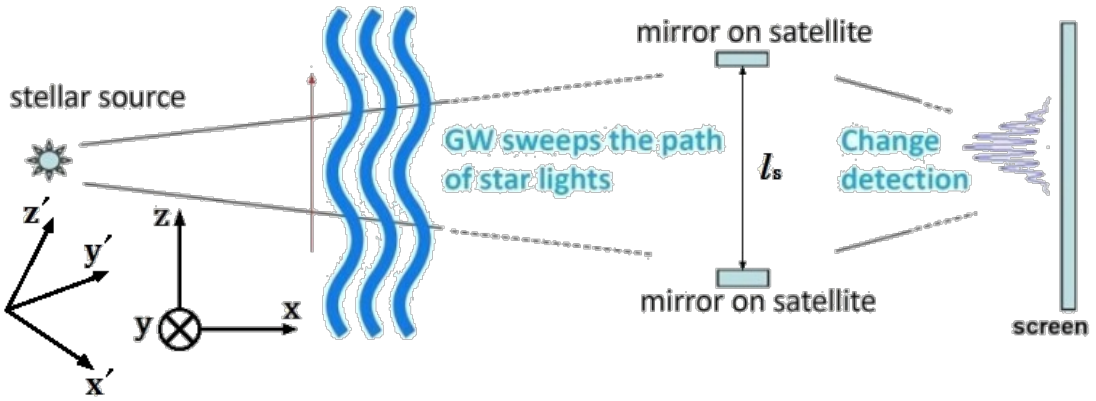

Shot noise

- A single photon creates an interference pattern but any attempt to see which slit the photon entered will destroy the interference pattern, otherwise the uncertainty principle would be violated.
  → $\Delta N_p \Delta\phi \sim 1$ (Uncertainty principle)
- $\Delta p\, \Delta x \sim \hbar/4\pi$ → $\Delta p = \Delta N \frac{\hbar}{\lambda}$ and $\Delta x = \delta L = hL_c$ (h: strain, Lc characteristic length of the SIGN and a wavelength of GW to be detected.) → $h = \frac{\lambda}{4\pi L_c}\frac{1}{\sqrt{N}}$
  - $N = P\frac{\lambda}{\hbar c}\tau$ (P is the optical power of a given star) → $\Delta N = \sqrt{N}$
  - Power $P_{m=8} \approx 10^{-10} W$ (note that available power for LISA $P_{LISA(available)} \approx 2 \times 10^{-10} W$)
  - $m = -\frac{5}{2} log_{10}(\frac{f}{f_0})$ where the reference flux $f_0 = 3.08 \times 10^{-20} \frac{erg}{s \cdot cm^2 \cdot Hz}$ for R-band with $\lambda = 0.64 \mu m$
- Then, minimum detectable change from the short noise for a star of mag=8, $\tau = 1$ and $\lambda = 100nm$ is $\boldsymbol{\delta L_{SIGN} = 10^{-12}\ m}$

Sensitivity of SIGN with shot noise

Then the sensitivity of SIGN is derived to

$$h_{\mathrm{SIGN}} = \left(\frac{\delta L_c}{L_c}\right) \cdot \left(\frac{L_c}{\ell_s}\right)$$
$$= \left(\frac{10^{-12}\ \mathrm{m}}{L_c}\right) \cdot \left(\frac{\lambda}{100\ \mathrm{nm}}\right)^{1/2} \cdot (2.5^{(8-\mathrm{mag})})^{1/2} \cdot \left(\frac{\tau}{1\ \mathrm{sec}}\right)^{-1/2} \cdot \left(\frac{L_c}{\ell_s}\right).$$

where the factor (Lc/ls) comes from the first-order detector response which reflects the fact that the separation between two satellites is not comparable to the wavelength of GW.

Acceleration noise

- Dominant at the low frequency range, below a few mHz.
  - For the case of LISA, this is the noise due to the acceleration on a test mass.
- Come from various sources of force involved, which is proportional to f^2.
- LISA Pathfinder launched in Dec 2015 to measure free-fall noise in space at frequency from 20 μHz to above 300 Hz.
  - The constant term in this noise is ~2×10^{-15} m $s^{-2}/\sqrt{\text{Hz}}$.

Acceleration noise estimate for LISA

Table 4.2 *Major sources of acceleration noise, and schemes to suppress their effects.*

Error Source	*Error**	*Number*	*Error Reduction Approach*
Thermal distortion of spacecraft	1	1	Carbon epoxy construction and limited power use variations
Thermal distortion of payload	0.5	1	Carbon-epoxy construction with $\alpha = 4 \times 10^{-7}$/K, plus two-stage thermal isolation of payload
Noise due to dielectric losses	1	1	Very low electrostatic coupling
Gravity noise due to spacecraft displacement	0.5	1	$1\,\mathrm{nm}/\sqrt{\mathrm{Hz}}$ control of spacecraft displacements with FEEP thrusters
Temperature difference variations across cavity	1	1	Three stages of thermal isolation plus symmetrical heat leak paths
Electrical force on charged proof mass	1	1	Small spacecraft displacements, > 1 mm position-sensor gaps, and discharging of proof mass
Lorentz force on charged proof mass from fluctuating interplanetary field	1	1	Intermittent discharging of proof mass, e.g. with UV light
Residual gas impacts on proof mass	1	1	Less than 3×10^{-7} Pa pressure in proof-mass cavity
Telescope thermal expansion	0.5	1	Low-expansion secondary mounting plus two-stage thermal isolation
Magnetic force on proof mass from fluctuating interplanetary field	0.5	1	10^{-6} proof-mass susceptibility plus moderate spacecraft magnetic-field gradient
Other substantial effects	0.5	4	
Other smaller effects	0.3	16	
Total effect of accelerations :	3	for one inertial sensor	
Effect in optical path :	**12**	$=$ variation in $\dfrac{\partial^2}{\partial t^2}\,(\mathcal{L}_2 - \mathcal{L}_1)$	

*) *Errors given in units of* $10^{-15}\,\mathrm{m\,s^{-2}}/\sqrt{\mathrm{Hz}}$

[LISA ppa2.08.pdf]

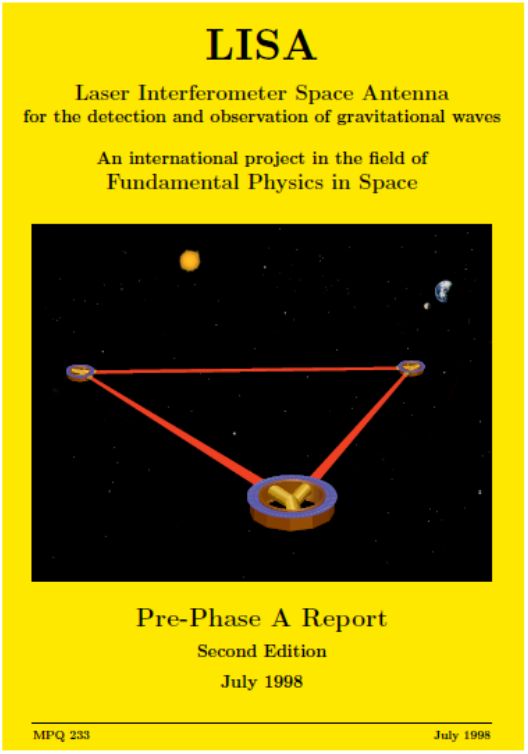

Acceleration noise

- Acceleration noise in SIGN be much lower than that of LISA
- SIGN will not host any test mass but a simple photodetector
- The orbital plane of satellites in SIGN is chosen to be perpendicular to the line of sight for a reference star. So potential forces resulting in acceleration noises in this direction would be small.

Δz is small
→ affect SIGN
$\Delta x, \Delta y$ large
→ not affect SIGN

Sensitivity of running and planned GW exps

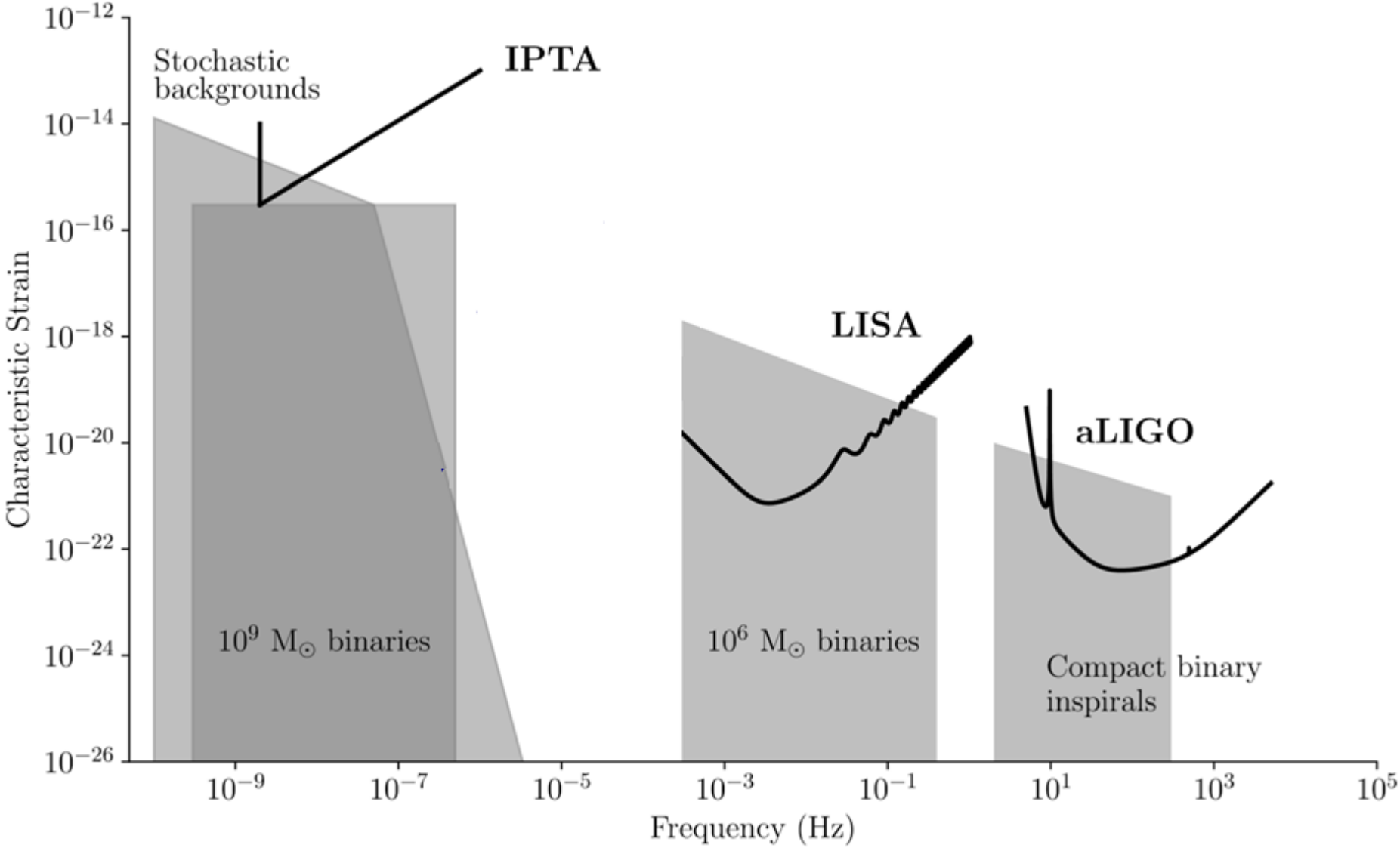

Sensitivity of running and planned GW exps

- 8-mag star, l_s=1,000 km, f_c=10^{-7}, 10^{-5}, 10^{-4} Hz (4 months, 2 days, 3 hours of t_{int})
- apply f^{-3} dependency for left wings from each f_c for acceleration noise and response function of SIGN.
- apply f^{2} dependency for right wings from each f_c for response function of SIGN.

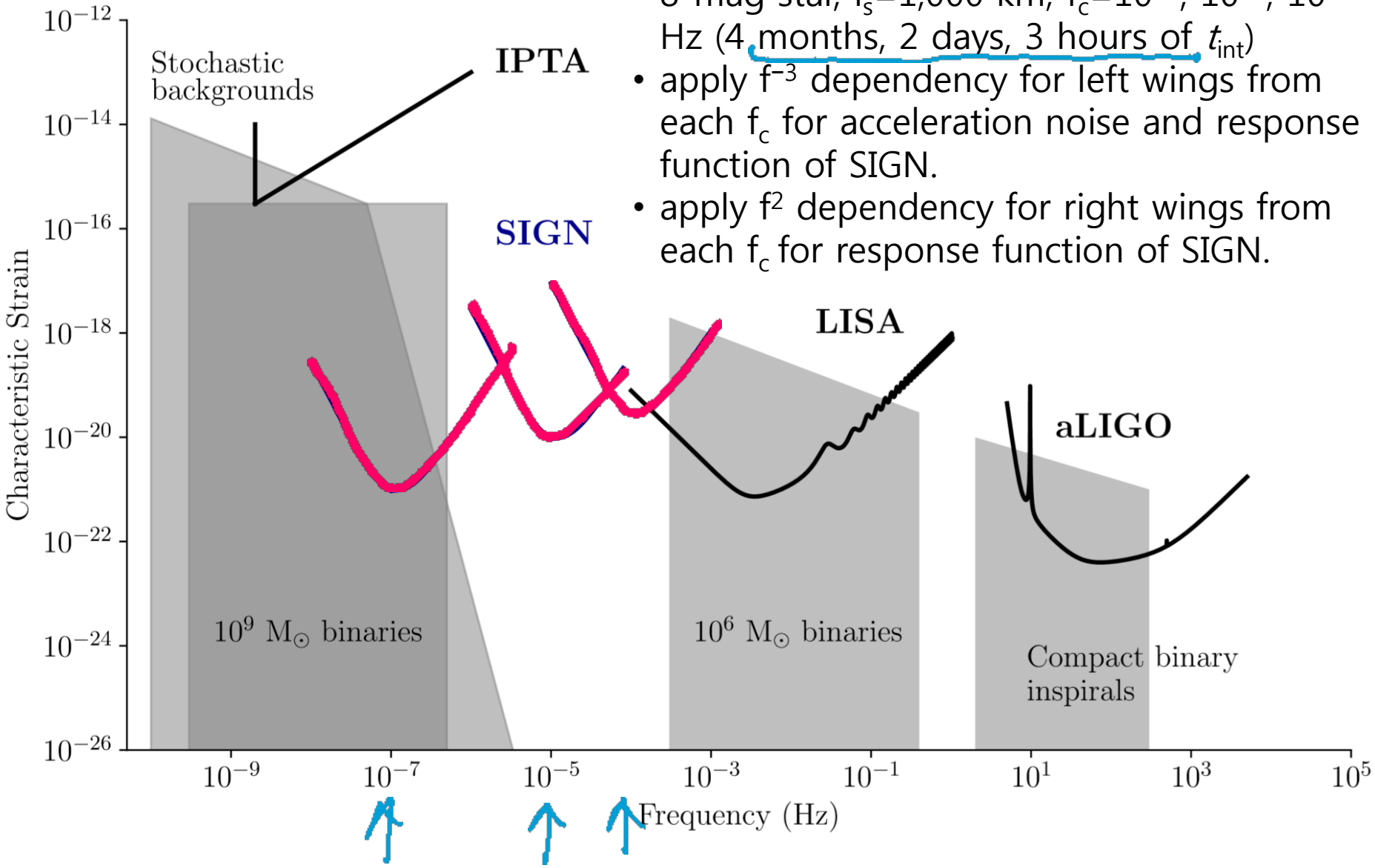

Sensitivity of running and planned GW exps

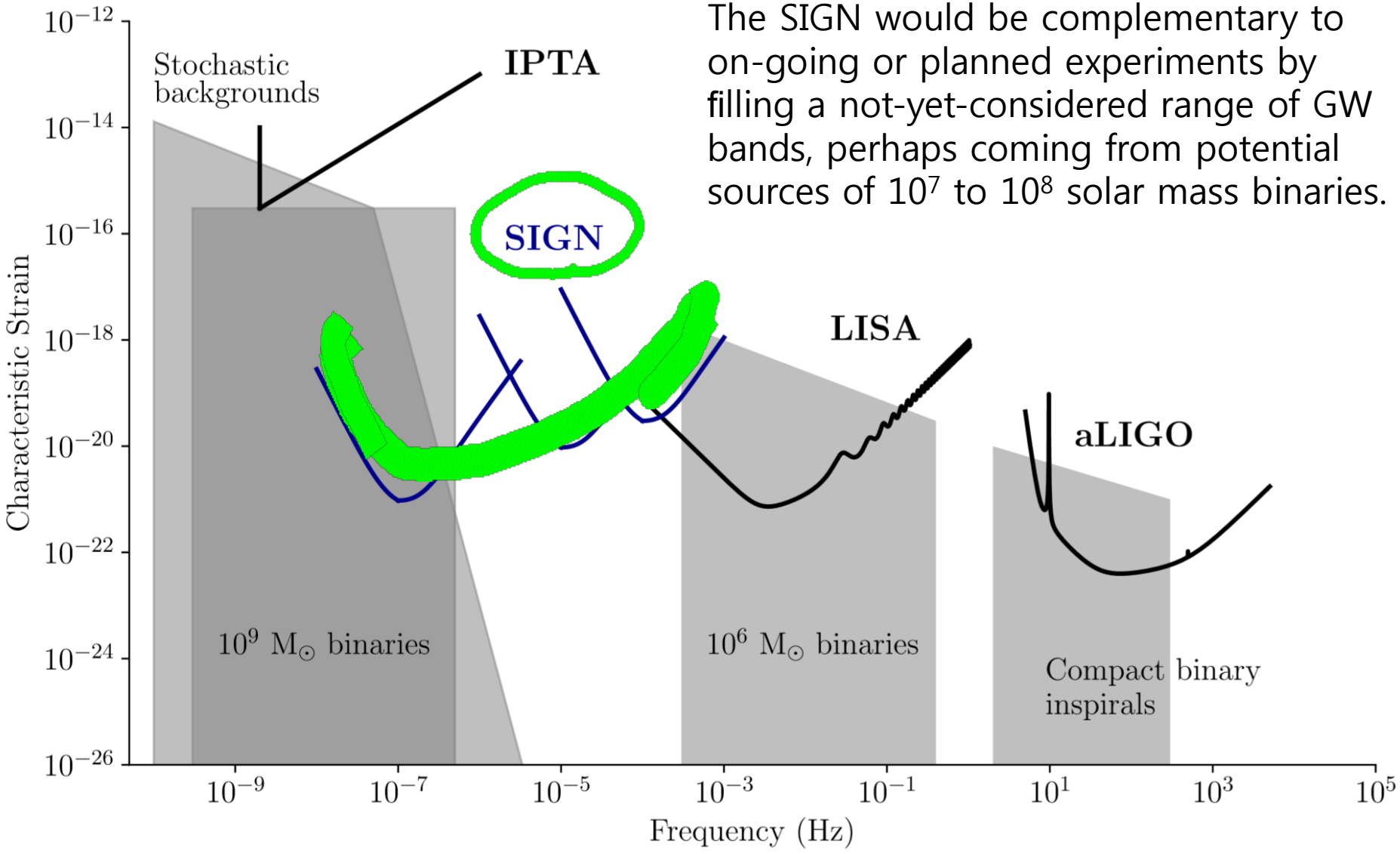

The SIGN would be complementary to on-going or planned experiments by filling a not-yet-considered range of GW bands, perhaps coming from potential sources of 10^7 to 10^8 solar mass binaries.

Technical challenge

- Pointing, stabilization & disturbance-free system
  - Interferometry: Track fringes to establish separation changes with 10pm accuracy
  - Inertial sensing: Sense deviations from inertial (geodesic) trajectories
  - Micro-newton thrusters: Mitigate against deviations from inertial trajectories owing to, e.g., acceleration noise from solar wind
- Maneuvering of satellites constellation
  - Tandem operation
  - Thrusters and fuel for long term operation in space
- Realization
  - Low cost: ~$60M depending on orbit chosen
  - Fast leadtime: 6 years after funding
  - A pathfinder experiment (or prototyping an idea) foreseen

Conclusion

- We propose a new method to detect GWs, based on the **space-based spatial coherence interferometry using star light** as opposed to conventional laser light.
- Two beams of light from a distant star are used in our space-borne experiment. In contrast to existing or proposed future gravitational wave detectors where the plane of two laser beams are located orthogonal to the propagation direction of gravitational waves at the maximum response to gravitational waves, our SIGN interferometer configures the direction of gravitational waves along the plane of two light beams. This configuration is expected to reduce noises in the low-frequency range significantly. → need SIGN-pathfinder mission
- For the SIGN experiment, important parameters include brightness, distance from us, size, and light bandwidth of a star.
- The SIGN would be complementary to existing GW detectors like laser interferometers and pulsar timing arrays, by **covering the frequency ranges of 10−7 −10−4 Hz of GWs**.

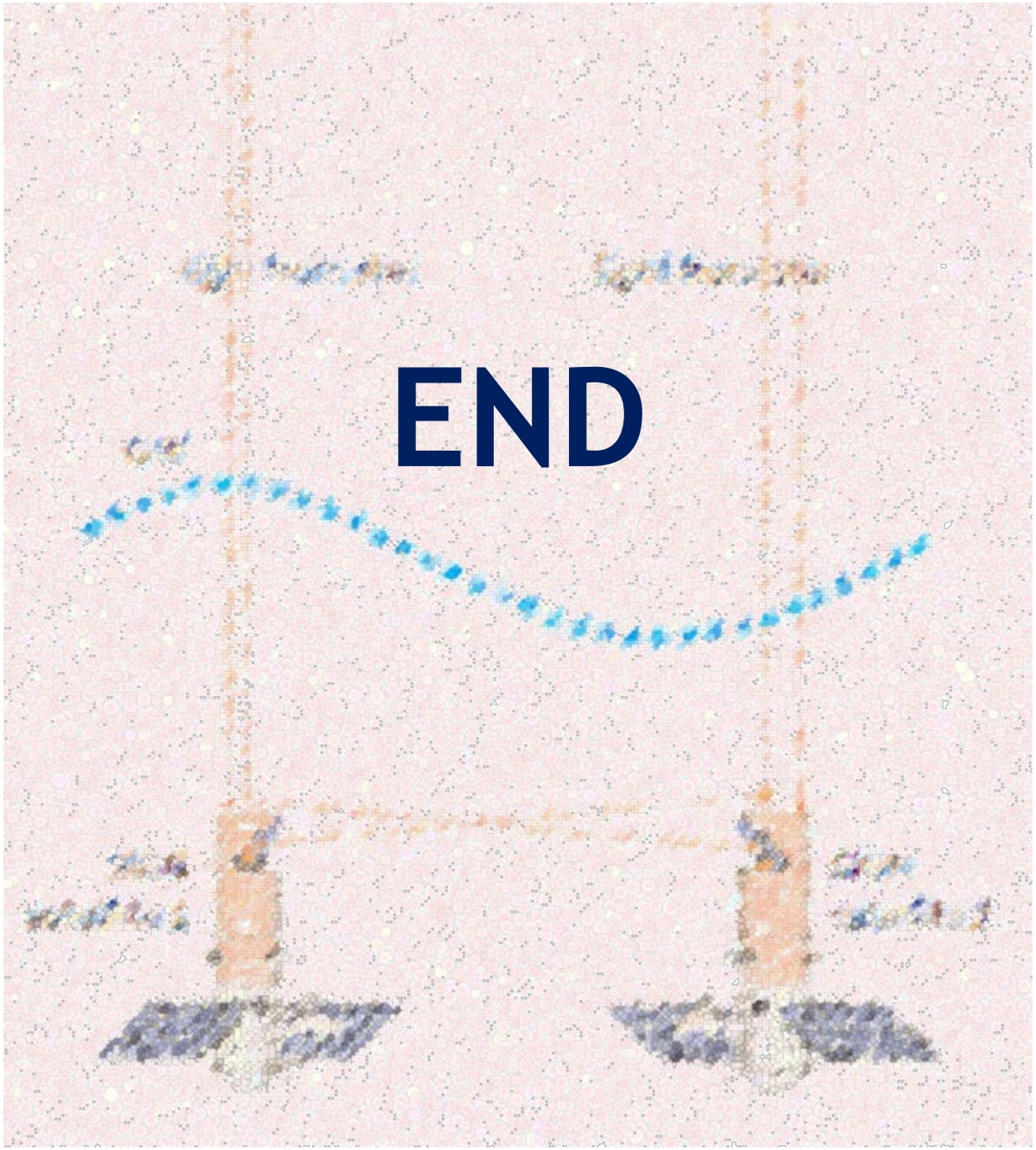
END

What about Intensity Interferometer

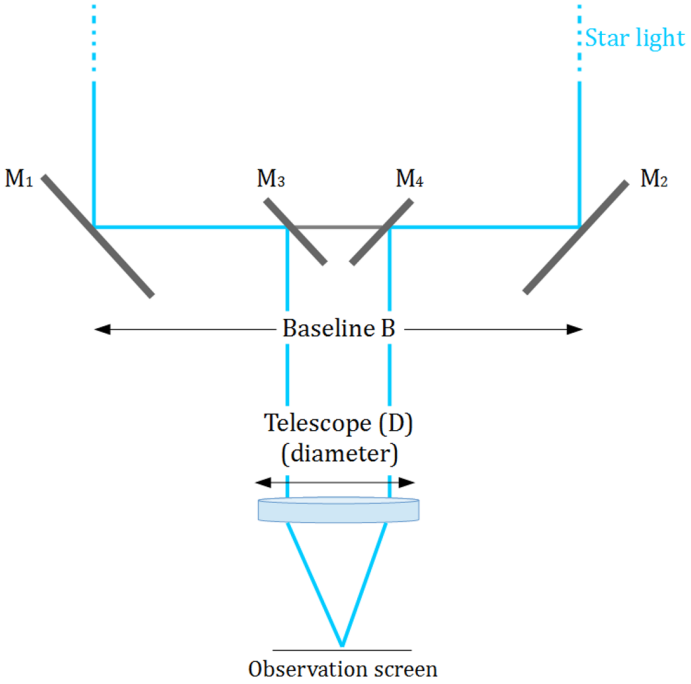

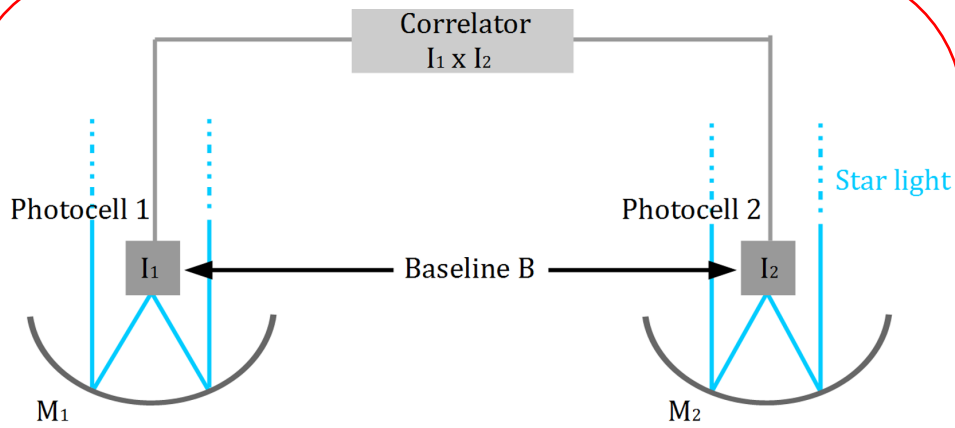

Stellar intensity interferometer. Two mirrors serve as light buckets and collect photons from a star. The intensity signal received at each photocell is converted into an electrical signal and sent to a correlator. The correlator multiplies the signal from the two detectors, providing the second-order coherence G(2). By changing the baseline B it is possible to retrieve a function similar to the visibility curve.